

Origin of Spin Stripes in Bilayer Nickelate $\text{La}_3\text{Ni}_2\text{O}_7$

Hao-Xin Wang,¹ Hanbit Oh,² Tobias Helbig,³ Bai Yang Wang,^{4,5} Jiarui Li,^{4,5} Yijun Yu,^{4,5} Harold Y. Hwang,^{4,5} Hong-Chen Jiang,⁴ Yi-Ming Wu,^{3,4,*} and S. Raghu^{3,4,†}

¹*Department of Physics, The Chinese University of Hong Kong, Sha Tin, New Territories, Hong Kong, China*

²*William H. Miller III Department of Physics and Astronomy,
Johns Hopkins University, Baltimore, Maryland, 21218, USA*

³*Leinweber Institute for Theoretical Physics, Stanford University, Stanford, CA 94305, USA*

⁴*Stanford Institute for Materials and Energy Sciences,*

SLAC National Accelerator Laboratory, Menlo Park, CA 94025, USA

⁵*Departments of Applied Physics, Stanford University, Stanford, CA 94305, USA*

The bilayer nickelate $\text{La}_3\text{Ni}_2\text{O}_7$ has emerged as a new high temperature superconductor. We propose and study a microscopic Hamiltonian that addresses the interplay of lattice structure and magnetism in this system. Using state-of-the-art density matrix renormalization group calculations, we show that $(\pi/2, \pi/2)$ spin stripe order emerges in our model and exhibits a hidden quasi-one dimensionality. The spin stripe order occurs over a range of electron concentrations, but requires a sizable Hund's coupling J_H . Our model exhibits superconducting tendency only when the interlayer antiferromagnetic coupling J_\perp becomes sufficiently large, which naturally occurs under pressure. Our study unveils the microscopic origin of both the unusual spin stripes and superconductivity in $\text{La}_3\text{Ni}_2\text{O}_7$, and highlights the indispensable role of Hund's coupling J_H in this system.

Introduction.—The Ruddlesden–Popper bilayer nickelate $\text{La}_3\text{Ni}_2\text{O}_7$ (LNO327) has emerged as a new type of high- T_c superconductor under high hydrostatic pressure, exhibiting transition temperatures as high as 80K [1–6]. At ambient pressure, an unusual type of spin stripe order (SSO) with momentum $\mathbf{Q} = (\pi/2, \pi/2)$ and onset temperature $T_{\text{SSO}} \approx 150\text{K}$ is observed instead, through various measurements including resonant inelastic X-ray scattering [7], μSR [8, 9], NMR [10, 11], and inelastic neutron scattering [12]. More recently, strain engineered thin films of $\text{La}_3\text{Ni}_2\text{O}_7$ at ambient pressure have also been shown to be superconducting ($T_c \approx 40\text{K}$) only if a sufficiently compressive strain is exerted [13–15], while without strain, the thin film sample again exhibits the $\mathbf{Q} = (\pi/2, \pi/2)$ SSO with similar T_{SSO} as in the bulk case [16, 17]. The thin film samples allow for easier access to the superconducting properties of this material, including the electronic structure from angle resolved photoemission spectroscopy (ARPES) [18–20] and scanning tunneling microscopy (STM) [21]. However, the pairing symmetry remains under debate, with competing proposals of s_\pm -wave and d -wave states [21–23].

Two indispensable ingredients in $\text{La}_3\text{Ni}_2\text{O}_7$ are essential for understanding the experimentally observed physics. The first one is the multi-orbital character due to the $3d^{7.5}$ electron configuration of the $\text{Ni}^{2.5+}$ cations: the active contributors to the electronic states are from d_{z^2} and $d_{x^2-y^2}$ orbitals, and the Hund's coupling J_H between them introduces another energy scale in addition to the onsite Coulomb repulsion, usually characterized by a Hubbard U . A second ingredient is the pressure/strain induced structural transition. At ambient pressure (or without strain for the thin film), $\text{La}_3\text{Ni}_2\text{O}_7$ has the space group $Amam$. A slice of the Ni-plane in this case is illustrated in Fig. 1(a), where the oxygen

atoms are buckled above and below the Ni-plane and the Ni-Ni bond length is non-uniform, resulting in a doubled unit cell. At higher pressure, the bulk structure changes to $Fmmm$, which is orthorhombic but nearly tetragonal, and may further change to tetragonal $I4/mmm$ at even higher pressure [24]. For the thin film sample with compressive strain, coupling to the substrate tends to enforce the $I4/mmm$ symmetry. Ref. [25] shows that both the bulk sample at high pressure and the thin film sample with compressive strain can be illustrated as in the right panel of Fig. 1(a). In this case, the Ni sites form a regular square lattice, and all the nearby oxygens are buckled in a uniform manner: thus, the high pressure (compressively strained) phase can be viewed as a bilayer square lattice. Given that superconductivity is observed only in the more symmetric high pressure (compressively strained) region, while the spin stripe develops in the less symmetric ambient pressure regime, it is crucial to understand the nature of these two regimes in a unified manner.

In this Letter, we address the origin of the spin stripe orders and superconductivity (SC) in $\text{La}_3\text{Ni}_2\text{O}_7$ by taking into account the impact from the crystal structural change. Although there have been proposals on the mechanism of the superconducting phase [26–67], a theoretical understanding of the formation of the $\mathbf{Q} = (\pi/2, \pi/2)$ spin order has remained a challenge [68–70]. Our starting point is the observation that the crystal structure in the ambient pressure $Amam$ case can be effectively described by a hopping non-uniformity $t' \neq t$ for the $d_{x^2-y^2}$ orbitals [equivalent to a (π, π) bond order], as shown in Fig. 1(b), while d_{z^2} orbitals provide local moments, which are coupled only through an interlayer J_\perp . Treating each layer separately, we have employed a large-scale density-matrix renormalization group (DMRG) cal-

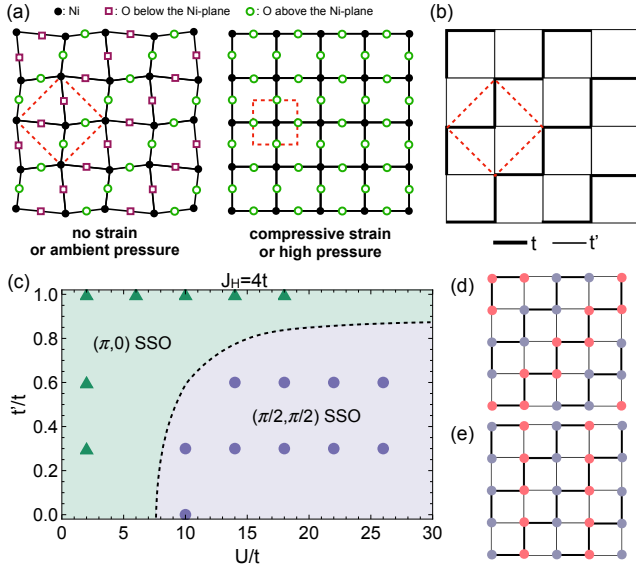


FIG. 1. (a) Illustration of a single Ni-O layer in the two phases which can be changed by strain. With tensile strain (and near zero strain), the positions of Ni atoms are distorted from a square lattice, while the O atoms are buckled either above or below the Ni-Ni plane. With large compressive strain, the Ni form a square lattice, with all O's buckled in the same direction. (b) In a minimal model that includes only the two e_g orbitals from Ni, the strain effect can be modeled by adding some anisotropy into the $d_{x^2-y^2}$ hopping, resulting in both strong (t) and weak (t') bonds. (c) Phase diagram of the model in Eq.(1) as a function of t' and U , for a particular $J_H = 4t$ and $J_\perp = 0$ obtained from DMRG calculation. The $(\pi/2, \pi/2)$ and $(\pi, 0)$ SSOs are shown in (d) and (e) respectively. Adding a small J_\perp makes the spin pattern opposite between the two layers.

ulation and obtained a phase diagram in the t' - U plane for a finite J_H , as shown in Fig. 1(c). The $(\pi/2, \pi/2)$ SSO consistent with experiments sets in only when $t' < t$ and U is sufficiently large. It admits a simple explanation: each one-dimensional (1D) 'zig-zag' chain with hopping t can be *ferromagnetic* due to double exchange from J_H [71, 72], and the weaker hopping t' induces an anti-ferromagnetic interchain coupling that eventually leads to the $(\pi/2, \pi/2)$ spin stripe pattern [see Fig. 1(d)]. In the symmetric case when $t' = t$, our DMRG calculation suggests that increasing J_\perp induces an interlayer s -wave pairing. Our study establishes a microscopic origin of both SSO and SC in $\text{La}_3\text{Ni}_2\text{O}_7$, highlighting the unique role of Hund's coupling in this new high- T_c material.

Model and method.—Due to the tetragonal elongation, the d_{z^2} orbitals from the Ni-sites have lower onsite energies than the $d_{x^2-y^2}$ orbitals [32]. Based on this, a microscopic calculation shows $\langle n_{x^2-y^2} \rangle = 1/2$ and $\langle n_{z^2} \rangle = 1$, i.e. the $d_{x^2-y^2}$ orbitals are quarter filled while the d_{z^2} orbitals are half filled. Namely, in the presence of strong interactions, the d_{z^2} orbitals form a Mott insulator while the $d_{x^2-y^2}$ orbitals provide itinerant fermions. The sys-

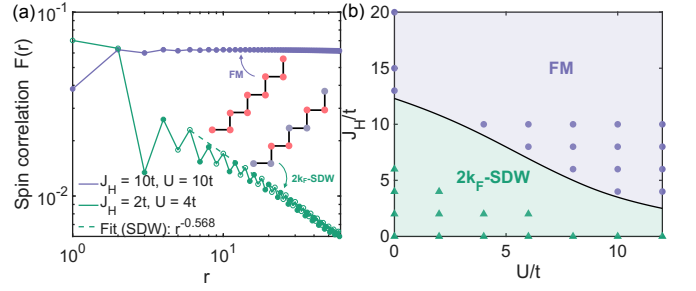


FIG. 2. (a) Representative spin correlation functions calculated from Eq. (2) for the FM and $2k_F$ -SDW phases, where the filled(hollow) markers in the data represent positive(negative) values. The inset shows the corresponding space patterns with the same color encoding as in Fig. 1(d,e). (b) Phase diagram for the model in Eq. (2) at quarter filling ($\langle n \rangle = 1/2$) determined by the spin correlation. The FM and $2k_F$ orders can be adiabatically connected to the $(\pi/2, \pi/2)$ and $(0, \pi)$ SDW orders respectively in the 2D limit.

tem is described by the following Hamiltonian[63]

$$\begin{aligned}
 H = & - \sum_{\langle ij \rangle, \ell, \sigma} \left(t_{ij} c_{i, \ell, \sigma}^\dagger c_{j, \ell, \sigma} + h.c. \right) + U \sum_{i\ell} n_{i\ell\uparrow} n_{i\ell\downarrow} \\
 & - J_H \sum_{i\ell} \mathbf{s}_{i, \ell} \cdot \mathbf{S}_{i, \ell} + J_\perp \sum_i \mathbf{S}_{i, 1} \cdot \mathbf{S}_{i, 2}.
 \end{aligned} \tag{1}$$

Here $\mathbf{s}_{i, \ell} = \frac{1}{2} \sum_{\alpha, \beta} c_{i, \ell, \alpha}^\dagger \boldsymbol{\sigma}_{\alpha\beta} c_{i, \ell, \beta}$ is the spin operator for the itinerant $d_{x^2-y^2}$ electrons at site i and layer ℓ with $\boldsymbol{\sigma}$ the vector of Pauli matrices. U is the Hubbard interaction for the itinerant electrons, $J_H > 0$ is the Hund's coupling and $J_\perp > 0$ is the interlayer super-exchange coupling between the local spins from the d_{z^2} orbitals. Only the nearest neighbor hoppings for $d_{x^2-y^2}$ orbitals are retained, and they are $t_{ij} = t$ on the strong bond, and $t_{ij} = t'$ on the weak bond, as shown in Fig. 1(b). Here $t' \neq t$ respects the *Amam* structure at ambient pressure, and $t' = t$ in the *I4/mmm* structure at high pressure (or with compressive strain in the thin film sample). Similar models with non-uniform hopping t_{ij} have also been used to study the impact of pressure on superconductivity in Ref.[73]. Below, we will assume that at ambient pressure (or in unstrained thin film), J_\perp is not strong enough to bind the pair of interlayer d_{z^2} orbitals into a singlet, such that the interlayer coupling can be treated perturbatively. This regime allows for a focus on one layer first, as the other layer is obtained by flipping the spin patterns. By contrast, in the high pressure regime, J_\perp cannot be treated perturbatively and the DMRG treatment must include both orbitals in both layers.

The ground state is investigated via GPU accelerated large-scale DMRG calculations [74] with a system size of up to 400 lattice sites, a bond dimension up to $D = 20000$ and truncation error of the order $\epsilon \sim 10^{-6}$. We employ the subspace expansion technique [75] while retaining the two-site update scheme to avoid local minima.

Decoupling limit.—Before discussing the spin stripes, it is helpful to first consider the artificial limit when $t' \rightarrow 0$, i.e. the hopping on the weak bonds vanishes. If we focus on a single layer by ignoring J_{\perp} , the system reduces to a 1D ‘zig-zag’ Kondo-Hubbard lattice along 45° -direction which is described by

$$H = -t \sum_{i,\sigma} c_{i\sigma}^{\dagger} c_{i+1\sigma} + h.c. + U \sum_i n_{i\uparrow} n_{i\downarrow} - J_H \sum_i \mathbf{s}_i \cdot \mathbf{S}_i \quad (2)$$

at $1/4$ filling. Much of the physics from this model is known when either U or J_H is absent.

The limit when J_H is negligible is just the 1D Hubbard model. It is well known from the Lieb-Mattis theorem [76, 77] that for the 1D Hubbard model, the ground state cannot be ferromagnetic at any finite filling and any strength U . Instead, the system tends to develop $2k_F$ density wave order. In the case of $1/4$ filling, $k_F = \frac{\pi}{4}$, and momentum $2k_F$ thus corresponds to period-4 commensurate density wave. Although both charge and spin density waves exhibit the same power-law correlation, spin ordering tendency is more favorable due to logarithmic corrections [78–80]. Thus, the ground state in this case is a period-4 $2k_F$ -SDW, as shown in the inset of Fig. 2(a).

In the other limit when U is negligible, the model reduces to the ferromagnetic Kondo model (also known as the double-exchange model) with J_H playing the role of the Kondo coupling. Interestingly, both the ferromagnetic ($J_H > 0$, see Refs. [81–84]) and antiferromagnetic ($J_H < 0$, see Refs. [85–93]) 1D Kondo lattice model feature a *ferromagnetic* ground state at large $|J_H|$ with conduction electron density $n \lesssim 0.8$. In the special limit $J_H \rightarrow \infty$, the ferromagnetic Kondo model is equivalent to spinless itinerant electrons [81, 83], where all the spins are polarized. We see from our calculation that the ferromagnetic Kondo model at $n = 1/2$ indeed favors the ferromagnetic ground state when $J_H \gtrsim 12t$, as shown in Fig. 2(b).

When J_H and U are both present, there is a competition between the $2k_F$ -SDW and ferromagnetic order. To reveal the ground state at arbitrary (J_H, U) , we performed DMRG calculation based on the one-dimensional model in Eq. (2). By calculating the spin-spin correlation of itinerant electron sites $F(|\mathbf{r}_i - \mathbf{r}_j|) = \langle \mathbf{s}_i \cdot \mathbf{s}_j \rangle$, we identified different ordering tendencies, which are shown in the phase diagram in Fig. 2(b). Two typical spin correlation functions are presented in Fig. 2(a), with the insets indicating their real space pattern. The correlation in the $2k_F$ -SDW state exhibits a power-law decay with a sign-change pattern of $++--$, whereas that in the FM state shows long-range order without decay and takes positive values throughout. For a given U , a large enough J_H will always drive the system into a ferromagnetic ground state. Since the superexchange process which requires virtual double occupancy and tends to destroy the FM ordering is suppressed at larger U , the critical J_H mark-

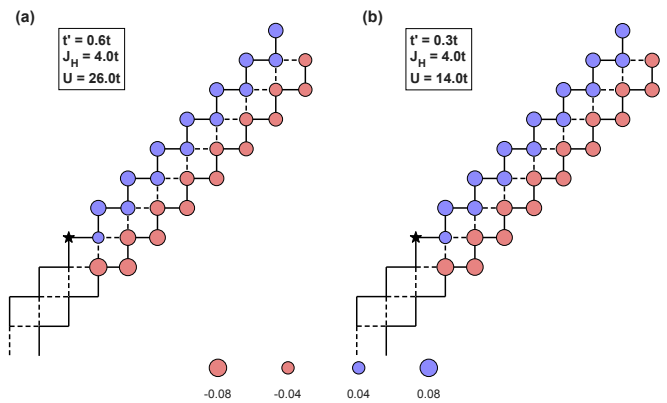


FIG. 3. Spin correlations from DMRG results where the decoupled 1D chains are in the ferromagnetic regime. The stars represent the reference sites. These correspond to a $(\pi/2, \pi/2)$ spin stripe in the 2D limit.

ing the onset of FM ordering is smaller with a larger U . Indeed, our numerical results indicate that the critical value of J_H decays with increasing U [see Fig. 2(b)].

Coupled two-chain system.—Having identified the ground states for the decoupled chain system, we now consider the crossover to the 2D case by switching on a small $t' \neq 0$ that couples the chains. We investigate the ground state of a coupled two-chain system by DMRG calculations, from which the 2D limit can be inferred. Before presenting the numerical results, some perturbative arguments in favor of the $(\pi/2, \pi/2)$ SSO are in order. Suppose the 1D system is in the ferromagnetic regime [see Fig. 2(b)], a small t' will induce anti-ferromagnetic coupling $J \sim t'^2/U$ between neighboring chains. In this case, the more energetically favorable state is when the spin polarization in each chain alternates from one to another, which eventually leads to a 2D $(\pi/2, \pi/2)$ SSO shown in Fig. 1(d). Our numerical results on the coupled two-chain system have indeed confirmed such a scenario. In Fig. 3 we show the calculated spin correlation function for two sets of representative parameters, and both show a pattern that is consistent with the 2D $(\pi/2, \pi/2)$ SSO. The regime in the t' - U plane that stabilizes this order for $J_H = 4t$ is shown in Fig. 1(c). We note that the SSO discussed here from coupling the ferromagnetic chain scenario crucially depends on the presence of a sizable J_H . We have confirmed numerically that by taking a smaller J_H , one needs a larger U to stabilize the stripe order. This is consistent with our 1D-limit results, where we see that for smaller J_H , the $2k_F$ order is favored and we need a larger U to obtain FM order. In the limit of $J_H \rightarrow 0$, the spin stripe of this kind would never arise, as we learn from Fig. 2(b) that each decoupled chain is in a $2k_F$ order without J_H .

There is another possible candidate for the $(\pi/2, \pi/2)$ SSO though, which may emerge in the absence of J_H . In this case, each decoupled chain is in the $2k_F$ order,

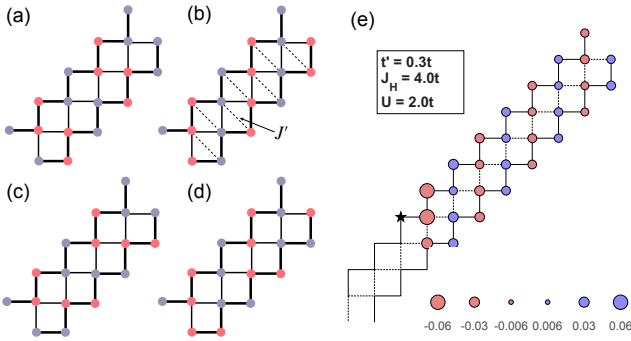


FIG. 4. (a-d) Four different possibilities of spin pattern in the coupled two-chain system when the decoupled 1D limit favors period-4 SDW tendency. Among them, (a) corresponds to another type of $(\pi/2, \pi/2)$ spin stripe, while (b) corresponds to a $(\pi, 0)$ spin stripe. Our DMRG results suggest the pattern in (b) is more stable, which can be explained through a fourth-order perturbation term $J' \sim t^2 t'^2 / U^3$ that couples diagonal sites in each square plaquette. (e) DMRG result for the spin correlation with $J_H = 4t$, $t' = 0.3t$, and $U = 2t$.

but the chains are coupled in the manner depicted in Fig. 4(a), consistent with a $(\pi/2, \pi/2)$ SSO in the 2D limit. This type of stripe order will be sensitive to the filling fraction of the $d_{x^2-y^2}$ orbitals, because it has momentum $(\pi/2, \pi/2)$ only when the $d_{x^2-y^2}$ orbitals are exactly at 1/4 filling. But more importantly, this state is not energetically favored. Consider the two chain system as in Fig. 4(a), and slide one chain relative to the other along the diagonal direction. This will lead to four different patterns shown in Fig. 4(a-d). If we only include the super-exchange coupling $J \sim t^2/U$ on the t' hopping bond, all the four patterns are equally frustrated. Moving beyond the second order perturbation, a fourth order exchange term $J' \sim (tt')^2/U^3$ which couples the chains along the plaquette diagonal direction is generated, and it is easy to see that the pattern in Fig. 4(b), which corresponds to a $(\pi, 0)$ SSO, has lower energy due to J' . Indeed from our DMRG calculation, we find a large parameter regime for this $(0, \pi)$ or $(\pi, 0)$ SSO at either smaller U or larger t' [see the green region in Fig. 1(c)]. The small U case confirms our analysis above. An example for such case is given in Fig. 4(e), which shows the calculated spin correlation function, implying a $(\pi, 0)$ order in the 2D limit. While for the $t' \rightarrow t$ case the picture of 1D chains coupled to each other breaks down since t' cannot be treated perturbatively.

Superconductivity at $t' = t$.—In the compressively strained thin film sample, or approximately in the bulk sample at high pressure where superconductivity is observed, the system retains tetragonal symmetry, implying $t' = t$ in our model. To inspect the ground state in this case, we perform DMRG calculations for the model in Eq. (1) with $t_{ij} = t$, on a regular square lattice with two layers, two orbitals and two legs (equivalent to an 8-leg problem in terms of computational com-

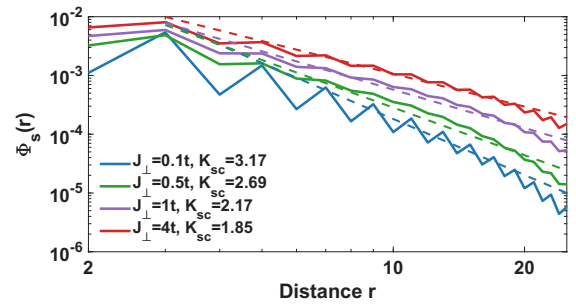


FIG. 5. Interlayer singlet pair correlation function $\Phi_s(\mathbf{r})$ calculated from Eq. (1) on a regular two layer, two leg and two orbital system for $J_H = 4t$, $U = 18t$.

plexity). Importantly, we explicitly include the interlayer exchange J_\perp , in contrast to the SSO calculation, where it was ignored and treated only perturbatively. This treatment is along with DFT calculations showing that J_\perp is enhanced at high pressure [73]. To detect evidence of a robust superconducting phase, we calculate the SC correlation $\Phi_s(\mathbf{r}) = \langle \Delta^\dagger(\mathbf{0})\Delta(\mathbf{r}) \rangle$, where $\Delta(\mathbf{r}_i) = (c_{i,1,\uparrow}c_{i,2,\downarrow} - c_{i,1,\downarrow}c_{i,2,\uparrow})/\sqrt{2}$ for interlayer singlet s -wave pairing [94]. The intralayer singlet pairing and interlayer triplet pairing are also investigated. However, we found that the intralayer pairing decays exponentially fast, while the interlayer triplet pairing is two-orders of magnitude smaller than the interlayer singlet pairing. Therefore, we focus on the interlayer singlet SC correlation $\Phi_s(\mathbf{r})$ defined above. In Fig. 5 we present the calculated $\Phi_s(\mathbf{r})$ for different values of J_\perp with other parameters fixed. It is clear that $\Phi_s(\mathbf{r})$ can exhibit power-law decay $r^{-K_{sc}}$ when the interlayer coupling J_\perp becomes large. Specifically, the exponent $K_{sc} < 2$ when $J_\perp = 4t$ for $J_H = 4t$, indicating the divergence of SC susceptibility. As J_\perp increases with pressure, our results indicate why pressure is essential in inducing pairing in this bilayer system. Our results are consistent with the previous results using effective one orbital model or type-II $t - J$ model [29, 31] considering $J_H \rightarrow \infty$, where similar s -wave pairing is also obtained.

Discussion.—Several candidate stripe orders have been proposed to explain the experimental data. In addition to the $(\pi/2, \pi/2)$ SSO discussed in our work [see Fig. 1(d)], another alternating spin-charge order also seems consistent with experiment in which Ni^{2+} and Ni^{3+} cations form alternating stripe structure and spin stripes only reside on the Ni^{2+} -stripe (see [7] for details, where our SSO is referred to as double spin stripe order). Ref. [7] also fitted the experimental data to the magnon dispersion calculated from an effective Heisenberg model and found agreement from both the spin-charge stripe and the double spin stripe orders. On the other hand, NMR measurement on the La-sites found no evidence of charge orders so far [10], probably due to the limit of sensitivity of charge orders on the La-atoms. From a symme-

try perspective, such a charge order with a momentum $\mathbf{q}_c = (\pi, \pi)$ is certainly allowed, and can actually be induced from the double spin stripe order. This can be seen from the following Ginzburg-Landau free energy

$$\mathcal{F} = \alpha |\rho_{\mathbf{q}_c}|^2 + \lambda [\rho_{\mathbf{q}_c} (S_{-\mathbf{Q}}^i)^2 + c.c.], \quad (3)$$

where $\alpha > 0$ meaning no spontaneous transition to the CDW order, and to preserve translational symmetry we must have $\mathbf{q}_c = 2\mathbf{Q}$. It is easy to see that with a finite $S_{\pm\mathbf{Q}}^i \neq 0$, \mathcal{F} is minimized at a nonzero charge order $\rho_{\mathbf{q}_c} = -\frac{\lambda}{\alpha} (S_{\mathbf{Q}}^i)^2$. Therefore, although we have found a double spin stripe order as the ground state, charge order can still set in as it obeys all the symmetries of the system and can be induced from spin stripes.

Acknowledgements.— We are grateful to Steven Kivelson, Zhengcheng Gu and Yahui Zhang for insightful discussions. H.O. is supported by a startup fund from Johns Hopkins University. T.H., Y.Y., H.H., H.-C.J., Y.W. and S.R. are supported by the US Department of Energy, Office of Basic Energy Sciences, Division of Materials Sciences and Engineering, under Contract No. DE-AC02-76SF00515. Y.W. acknowledges support from the Gordon and Betty Moore Foundation’s EPIQS Initiative through GBMF8686. T.H. was supported by the Deutsche Forschungsgemeinschaft (DFG, German Research Foundation) under Project No. 537357978.

* yimwu@stanford.edu

† sraghu@stanford.edu

- [1] H. Sun, M. Huo, X. Hu, J. Li, Z. Liu, Y. Han, L. Tang, Z. Mao, P. Yang, B. Wang, J. Cheng, D.-X. Yao, G.-M. Zhang, and M. Wang, Signatures of superconductivity near 80 K in a nickelate under high pressure, *Nature* **621**, 493 (2023).
- [2] Y. Zhang, D. Su, Y. Huang, Z. Shan, H. Sun, M. Huo, K. Ye, J. Zhang, Z. Yang, Y. Xu, Y. Su, R. Li, M. Smidman, M. Wang, L. Jiao, and H. Yuan, High-temperature superconductivity with zero-resistance and strange metal behavior in $\text{La}_3\text{Ni}_2\text{O}_{7-\delta}$, *Nature Physics* **20**, 1269 (2024).
- [3] J. Hou, P.-T. Yang, Z.-Y. Liu, J.-Y. Li, P.-F. Shan, L. Ma, G. Wang, N.-N. Wang, H.-Z. Guo, J.-P. Sun, Y. Uwatoko, M. Wang, G.-M. Zhang, B.-S. Wang, and J.-G. Cheng, Emergence of High-Temperature Superconducting Phase in Pressurized $\text{La}_3\text{Ni}_2\text{O}_7$ Crystals, *Chinese Physics Letters* **40**, 117302 (2023).
- [4] Z. Liu, M. Huo, J. Li, Q. Li, Y. Liu, Y. Dai, X. Zhou, J. Hao, Y. Lu, M. Wang, and H.-H. Wen, Electronic correlations and partial gap in the bilayer nickelate $\text{La}_3\text{Ni}_2\text{O}_7$, *Nature Communications* **15**, 7570 (2024).
- [5] J. Yang, H. Sun, X. Hu, Y. Xie, T. Miao, H. Luo, H. Chen, B. Liang, W. Zhu, G. Qu, C.-Q. Chen, M. Huo, Y. Huang, S. Zhang, F. Zhang, F. Yang, Z. Wang, Q. Peng, H. Mao, G. Liu, Z. Xu, T. Qian, D.-X. Yao, M. Wang, L. Zhao, and X. J. Zhou, Orbital-dependent electron correlation in double-layer nickelate $\text{La}_3\text{Ni}_2\text{O}_7$, *Nature Communications* **15**, 4373 (2024).
- [6] M. Zhang, C. Pei, Q. Wang, Y. Zhao, C. Li, W. Cao, S. Zhu, J. Wu, and Y. Qi, Effects of pressure and doping on Ruddlesden-Popper phases $\text{La}_{n+1}\text{Ni}_n\text{O}_{3n+1}$, *Journal of Materials Science & Technology* **185**, 147 (2024).
- [7] X. Chen, J. Choi, Z. Jiang, J. Mei, K. Jiang, J. Li, S. Agrestini, M. Garcia-Fernandez, H. Sun, X. Huang, D. Shen, M. Wang, J. Hu, Y. Lu, K.-J. Zhou, and D. Feng, Electronic and magnetic excitations in $\text{La}_3\text{Ni}_2\text{O}_7$, *Nature Communications* **15**, 9597 (2024).
- [8] K. Chen, X. Liu, J. Jiao, M. Zou, C. Jiang, X. Li, Y. Luo, Q. Wu, N. Zhang, Y. Guo, and L. Shu, Evidence of Spin Density Waves in $\text{La}_3\text{Ni}_2\text{O}_{7-\delta}$, *Phys. Rev. Lett.* **132**, 256503 (2024).
- [9] R. Khasanov, T. J. Hicken, D. J. Gawryluk, V. Sazgari, I. Plokhikh, L. P. Sorel, M. Bartkowiak, S. Bötzel, F. Lechermann, I. M. Eremin, H. Luetkens, and Z. Guguchia, Pressure-enhanced splitting of density wave transitions in $\text{La}_3\text{Ni}_2\text{O}_{7-\delta}$, *Nature Physics* **21**, 430 (2025).
- [10] D. Zhao, Y. Zhou, M. Huo, Y. Wang, L. Nie, Y. Yang, J. Ying, M. Wang, T. Wu, and X. Chen, Pressure-enhanced spin-density-wave transition in double-layer nickelate $\text{La}_3\text{Ni}_2\text{O}_{7-\delta}$, *Science Bulletin* **70**, 1239 (2025).
- [11] M. Kakoi, T. Oi, Y. Ohshita, M. Yashima, K. Kuroki, T. Kato, H. Takahashi, S. Ishiwata, Y. Adachi, N. Hatada, *et al.*, Multiband metallic ground state in multilayered nickelates $\text{La}_3\text{Ni}_2\text{O}_7$ and $\text{La}_4\text{Ni}_3\text{O}_{10}$ probed by ^{139}La -NMR at ambient pressure, *Journal of the Physical Society of Japan* **93**, 053702 (2024).
- [12] T. Xie, M. Huo, X. Ni, F. Shen, X. Huang, H. Sun, H. C. Walker, D. Adroja, D. Yu, B. Shen, L. He, K. Cao, and M. Wang, Strong interlayer magnetic exchange coupling in $\text{La}_3\text{Ni}_2\text{O}_{7-\delta}$ revealed by inelastic neutron scattering, *Science Bulletin* **69**, 3221 (2024).
- [13] E. K. Ko, Y. Yu, Y. Liu, L. Bhatt, J. Li, V. Thampy, C.-T. Kuo, B. Y. Wang, Y. Lee, K. Lee, J.-S. Lee, B. H. Goodge, D. A. Muller, and H. Y. Hwang, Signatures of ambient pressure superconductivity in thin film $\text{La}_3\text{Ni}_2\text{O}_7$, *Nature* [10.1038/s41586-024-08525-3](https://doi.org/10.1038/s41586-024-08525-3) (2024).
- [14] G. Zhou, W. Lv, H. Wang, Z. Nie, Y. Chen, Y. Li, H. Huang, W.-Q. Chen, Y.-J. Sun, Q.-K. Xue, and Z. Chen, Ambient-pressure superconductivity onset above 40 K in $(\text{La},\text{Pr})_3\text{Ni}_2\text{O}_7$ films, *Nature* **640**, 641 (2025).
- [15] Y. Liu, E. K. Ko, Y. Tarn, L. Bhatt, J. Li, V. Thampy, B. H. Goodge, D. A. Muller, S. Raghu, Y. Yu, and H. Y. Hwang, Superconductivity and normal-state transport in compressively strained $\text{La}_2\text{PrNi}_2\text{O}_7$ thin films, *Nature Materials* **24**, 1221 (2025).
- [16] N. K. Gupta, R. Gong, Y. Wu, M. Kang, C. T. Parzyck, B. Z. Gregory, N. Costa, R. Sutarto, S. Sarker, A. Singer, D. G. Schlom, K. M. Shen, and D. G. Hawthorn, Anisotropic spin stripe domains in bilayer $\text{La}_3\text{Ni}_2\text{O}_7$, *Nature Communications* **16**, 6560 (2025).
- [17] X. Ren, R. Sutarto, X. Wu, J. Zhang, H. Huang, T. Xiang, J. Hu, R. Comin, X. Zhou, and Z. Zhu, Resolving the electronic ground state of $\text{La}_3\text{Ni}_2\text{O}_{7-\delta}$ films, *Communications Physics* **8**, 52 (2025).
- [18] P. Li, G. Zhou, W. Lv, Y. Li, C. Yue, H. Huang, L. Xu, J. Shen, Y. Miao, W. Song, Z. Nie, Y. Chen, H. Wang, W. Chen, Y. Huang, Z.-H. Chen, T. Qian, J. Lin, J. He, Y.-J. Sun, Z. Chen, and Q.-K. Xue, Angle-resolved photoemission spectroscopy of superconducting $(\text{La},\text{Pr})_3\text{Ni}_2\text{O}_7/\text{SrLaAlO}_4$ heterostructures, Na-

- tional Science Review [10.1093/nsr/nwaf205](https://doi.org/10.1093/nsr/nwaf205) (2025).
- [19] C. Yue, J.-J. Miao, H. Huang, Y. Hua, P. Li, Y. Li, G. Zhou, W. Lv, Q. Yang, H. Sun, Y.-J. Sun, J. Lin, Q.-K. Xue, Z. Chen, and W.-Q. Chen, [Correlated electronic structures and unconventional superconductivity in bilayer nickelate heterostructures](#) (2025), [arXiv:2501.06875 \[cond-mat.str-el\]](https://arxiv.org/abs/2501.06875).
- [20] B. Y. Wang, Y. Zhong, S. Abadi, Y. Liu, Y. Yu, X. Zhang, Y.-M. Wu, R. Wang, J. Li, Y. Tarn, E. K. Ko, V. Thampy, M. Hashimoto, D. Lu, Y. S. Lee, T. P. Devereaux, C. Jia, H. Y. Hwang, and Z.-X. Shen, [Electronic structure of compressively strained thin film \$\text{La}_2\text{PrNi}_2\text{O}_7\$](#) (2025), [arXiv:2504.16372 \[cond-mat.supr-con\]](https://arxiv.org/abs/2504.16372).
- [21] S. Fan, M. Ou, M. Scholten, Q. Li, Z. Shang, Y. Wang, J. Xu, H. Yang, I. M. Eremin, and H.-H. Wen, [Superconducting gap structure and bosonic mode in \$\text{La}_2\text{PrNi}_2\text{O}_7\$ thin films at ambient pressure](#) (2025), [arXiv:2506.01788 \[cond-mat.supr-con\]](https://arxiv.org/abs/2506.01788).
- [22] J. Guo, Y. Chen, Y. Wang, H. Sun, D. Hu, M. Wang, X. Huang, and T. Cui, [Revealing superconducting gap in \$\text{La}_3\text{Ni}_2\text{O}_7-\delta\$ by andreev reflection spectroscopy under high pressure](#) (2025), [arXiv:2509.12601 \[cond-mat.supr-con\]](https://arxiv.org/abs/2509.12601).
- [23] Z.-Y. Cao, D. Peng, S. Choi, F. Lan, L. Yu, E. Zhang, Z. Xing, Y. Liu, F. Zhang, T. Luo, L. Chen, V. T. A. Hong, S.-Y. Paek, H. Jang, J. Xie, H. Liu, H. Lou, Z. Zeng, Y. Ding, J. Zhao, C. Liu, T. Park, Q. Zeng, and H. kwang Mao, [Direct observation of d-wave superconducting gap symmetry in pressurized \$\text{La}_3\text{Ni}_2\text{O}_7\$ single crystals](#) (2025), [arXiv:2509.12606 \[cond-mat.supr-con\]](https://arxiv.org/abs/2509.12606).
- [24] L. Wang, Y. Li, S.-Y. Xie, F. Liu, H. Sun, C. Huang, Y. Gao, T. Nakagawa, B. Fu, B. Dong, Z. Cao, R. Yu, S. I. Kawaguchi, H. Kadobayashi, M. Wang, C. Jin, H.-k. Mao, and H. Liu, [Structure Responsible for the Superconducting State in \$\text{La}_3\text{Ni}_2\text{O}_7\$ at High-Pressure and Low-Temperature Conditions](#), *Journal of the American Chemical Society* **146**, 7506 (2024).
- [25] L. Bhatt, A. Y. Jiang, E. K. Ko, N. Schnitzer, G. A. Pan, D. F. Segedin, Y. Liu, Y. Yu, Y.-F. Zhao, E. A. Morales, C. M. Brooks, A. S. Botana, H. Y. Hwang, J. A. Mundy, D. A. Muller, and B. H. Goodge, [Resolving structural origins for superconductivity in strain-engineered \$\text{La}_3\text{Ni}_2\text{O}_7\$ thin films](#) (2025), [arXiv:2501.08204 \[cond-mat.supr-con\]](https://arxiv.org/abs/2501.08204).
- [26] Q.-G. Yang, D. Wang, and Q.-H. Wang, [Possible \$s_{\pm}\$ -wave superconductivity in \$\text{La}_3\text{Ni}_2\text{O}_7\$](#) , *Phys. Rev. B* **108**, L140505 (2023).
- [27] Y.-f. Yang, G.-M. Zhang, and F.-C. Zhang, [Interlayer valence bonds and two-component theory for high- \$T_c\$ superconductivity of \$\text{La}_3\text{Ni}_2\text{O}_7\$ under pressure](#), *Phys. Rev. B* **108**, L201108 (2023).
- [28] C. Lu, Z. Pan, F. Yang, and C. Wu, [Interlayer-Coupling-Driven High-Temperature Superconductivity in \$\text{La}_3\text{Ni}_2\text{O}_7\$ under Pressure](#), *Phys. Rev. Lett.* **132**, 146002 (2024).
- [29] X.-Z. Qu, D.-W. Qu, J. Chen, C. Wu, F. Yang, W. Li, and G. Su, [Bilayer \$t-J-J_{\perp}\$ Model and Magnetically Mediated Pairing in the Pressurized Nickelate \$\text{La}_3\text{Ni}_2\text{O}_7\$](#) , *Phys. Rev. Lett.* **132**, 036502 (2024).
- [30] H. Oh and Y.-H. Zhang, [Type-II \$t-J\$ model and shared superexchange coupling from Hund's rule in superconducting \$\text{La}_3\text{Ni}_2\text{O}_7\$](#) , *Phys. Rev. B* **108**, 174511 (2023).
- [31] H. Yang, H. Oh, and Y.-H. Zhang, [Strong pairing from a small Fermi surface beyond weak coupling: Application to \$\text{La}_3\text{Ni}_2\text{O}_7\$](#) , *Phys. Rev. B* **110**, 104517 (2024).
- [32] Z. Luo, X. Hu, M. Wang, W. Wú, and D.-X. Yao, [Bilayer two-orbital model of \$\text{La}_3\text{Ni}_2\text{O}_7\$ under pressure](#), *Phys. Rev. Lett.* **131**, 126001 (2023).
- [33] Y. Gu, C. Le, Z. Yang, X. Wu, and J. Hu, [Effective model and pairing tendency in the bilayer Ni-based superconductor \$\text{La}_3\text{Ni}_2\text{O}_7\$](#) , *Phys. Rev. B* **111**, 174506 (2025).
- [34] Y. Shen, M. Qin, and G.-M. Zhang, [Effective bi-layer model Hamiltonian and density-matrix renormalization group study for the high- \$T_c\$ superconductivity in \$\text{La}_3\text{Ni}_2\text{O}_7\$ under high pressure](#), *Chinese Physics Letters* **40**, 127401 (2023).
- [35] W. Wú, Z. Luo, D.-X. Yao, and M. Wang, [Superexchange and charge transfer in the nickelate superconductor \$\text{La}_3\text{Ni}_2\text{O}_7\$ under pressure](#), *Science China Physics, Mechanics & Astronomy* **67**, 117402 (2024).
- [36] H. Oh, B. Zhou, and Y.-H. Zhang, [Type-II \$t-J\$ model in charge transfer regime in bilayer \$\text{La}_3\text{Ni}_2\text{O}_7\$ and trilayer \$\text{La}_4\text{Ni}_3\text{O}_{10}\$](#) , *Phys. Rev. B* **111**, L020504 (2025).
- [37] V. Christiansson, F. Petocchi, and P. Werner, [Correlated Electronic Structure of \$\text{La}_3\text{Ni}_2\text{O}_7\$ under Pressure](#), *Phys. Rev. Lett.* **131**, 206501 (2023).
- [38] Y.-B. Liu, J.-W. Mei, F. Ye, W.-Q. Chen, and F. Yang, [\$s^{\pm}\$ -Wave Pairing and the Destructive Role of Apical-Oxygen Deficiencies in \$\text{La}_3\text{Ni}_2\text{O}_7\$ under Pressure](#), *Phys. Rev. Lett.* **131**, 236002 (2023).
- [39] Y. Cao and Y.-f. Yang, [Flat bands promoted by Hund's rule coupling in the candidate double-layer high-temperature superconductor \$\text{La}_3\text{Ni}_2\text{O}_7\$ under high pressure](#), *Phys. Rev. B* **109**, L081105 (2024).
- [40] D.-C. Lu, M. Li, Z.-Y. Zeng, W. Hou, J. Wang, F. Yang, and Y.-Z. You, [Superconductivity from Doping Symmetric Mass Generation Insulators: Application to \$\text{La}_3\text{Ni}_2\text{O}_7\$ under Pressure](#), [arXiv preprint arXiv:2308.11195](https://arxiv.org/abs/2308.11195) (2023).
- [41] R. Jiang, J. Hou, Z. Fan, Z.-J. Lang, and W. Ku, [Pressure Driven Fractionalization of Ionic Spins Results in Cupratelike High- \$T_c\$ Superconductivity in \$\text{La}_3\text{Ni}_2\text{O}_7\$](#) , *Phys. Rev. Lett.* **132**, 126503 (2024).
- [42] Y.-H. Tian, Y. Chen, J.-M. Wang, R.-Q. He, and Z.-Y. Lu, [Correlation effects and concomitant two-orbital \$s_{\pm}\$ -wave superconductivity in \$\text{La}_3\text{Ni}_2\text{O}_7\$ under high pressure](#) (2024).
- [43] J.-X. Zhang, H.-K. Zhang, Y.-Z. You, and Z.-Y. Weng, [Strong Pairing Originated from an Emergent \$\mathbb{Z}_2\$ Berry Phase in \$\text{La}_3\text{Ni}_2\text{O}_7\$](#) , *Phys. Rev. Lett.* **133**, 126501 (2024).
- [44] Q. Qin and Y.-f. Yang, [High- \$T_c\$ superconductivity by mobilizing local spin singlets and possible route to higher \$T_c\$ in pressurized \$\text{La}_3\text{Ni}_2\text{O}_7\$](#) , *Phys. Rev. B* **108**, L140504 (2023).
- [45] J. Huang, Z. D. Wang, and T. Zhou, [Impurity and vortex states in the bilayer high-temperature superconductor \$\text{La}_3\text{Ni}_2\text{O}_7\$](#) , *Phys. Rev. B* **108**, 174501 (2023).
- [46] Y. Zhang, L.-F. Lin, A. Moreo, T. A. Maier, and E. Dagotto, [Trends in electronic structures and \$s_{\pm}\$ -wave pairing for the rare-earth series in bilayer nickelate superconductor \$R_3\text{Ni}_2\text{O}_7\$](#) , *Phys. Rev. B* **108**, 165141 (2023).
- [47] N. Kitamine, M. Ochi, and K. Kuroki, [Theoretical designing of multiband Nickelate and Palladate superconductors with \$d^{8+\delta}\$ configuration](#), [arXiv e-prints](https://arxiv.org/abs/2308.12750), [arXiv:2308.12750](https://arxiv.org/abs/2308.12750) (2023), [arXiv:2308.12750 \[cond-mat.supr-con\]](https://arxiv.org/abs/2308.12750).
- [48] H. Lange, L. Homeier, E. Demler, U. Schollwöck, A. Bohrdt, and F. Grusdt, [Pairing dome from an emergent feshbach resonance in a strongly repulsive bilayer model](#), *Phys. Rev. B* **110**, L081113 (2024).

- [49] H. Lange, L. Homeier, E. Demler, U. Schollwöck, F. Grusdt, and A. Bohrdt, Feshbach resonance in a strongly repulsive bilayer model: a possible scenario for bilayer nickelate superconductors (2023), [arXiv:2309.15843 \[cond-mat.str-el\]](#).
- [50] H. Schlömer, U. Schollwöck, F. Grusdt, and A. Bohrdt, Superconductivity in the pressurized nickelate $\text{La}_3\text{Ni}_2\text{O}_7$ in the vicinity of a BEC-BCS crossover (2023), [arXiv:2311.03349 \[cond-mat.str-el\]](#).
- [51] J. Zhan, Y. Gu, X. Wu, and J. Hu, Cooperation between electron-phonon coupling and electronic interaction in bilayer nickelates $\text{La}_3\text{Ni}_2\text{O}_7$ (2024), [arXiv:2404.03638 \[cond-mat.supr-con\]](#).
- [52] F. Lechermann, S. Bötzel, and I. M. Eremin, Electronic instability, layer selectivity, and Fermi arcs in $\text{La}_3\text{Ni}_2\text{O}_7$, *Phys. Rev. Mater.* **8**, 074802 (2024).
- [53] G. Wang, N. Wang, X. Shen, J. Hou, L. Ma, L. Shi, Z. Ren, Y. Gu, H. Ma, P. Yang, *et al.*, Pressure-induced superconductivity in polycrystalline $\text{La}_3\text{Ni}_2\text{O}_{7-\delta}$, *Physical Review X* **14**, 011040 (2024).
- [54] J.-R. Xue and F. Wang, Magnetism and Superconductivity in the t-J Model of $\text{La}_3\text{Ni}_2\text{O}_7$ Under Multiband Gutzwiller Approximation, *Chinese Physics Letters* **41**, 057403 (2024).
- [55] Y. Zhang, L.-F. Lin, A. Moreo, T. A. Maier, and E. Dagotto, Structural phase transition, $s\pm$ -wave pairing, and magnetic stripe order in bilayered superconductor $\text{La}_3\text{Ni}_2\text{O}_7$ under pressure, *Nature Communications* **15**, 2470 (2024).
- [56] K. Jiang, Z. Wang, and F.-C. Zhang, High-temperature superconductivity in $\text{La}_3\text{Ni}_2\text{O}_7$, *Chinese Physics Letters* **41**, 017402 (2024).
- [57] Z. Liao, L. Chen, G. Duan, Y. Wang, C. Liu, R. Yu, and Q. Si, Electron correlations and superconductivity in $\text{La}_3\text{Ni}_2\text{O}_7$ under pressure tuning, *Phys. Rev. B* **108**, 214522 (2023).
- [58] H. Oh, Y.-M. Wu, J. May-Mann, Y. Yu, H. Y. Hwang, Y.-H. Zhang, and S. Raghu, *High spin, low spin or gapped spins: magnetism in the bilayer nickelates* (2025), [arXiv:2506.18973 \[cond-mat.str-el\]](#).
- [59] B. Geisler, L. Fanfarillo, J. J. Hamlin, G. R. Stewart, R. G. Hennig, and P. J. Hirschfeld, Optical properties and electronic correlations in $\text{La}_3\text{Ni}_2\text{O}_7$ bilayer nickelates under high pressure, *npj Quantum Materials* **9**, 89 (2024).
- [60] B. Geisler, J. J. Hamlin, G. R. Stewart, R. G. Hennig, and P. J. Hirschfeld, *Electronic reconstruction and interface engineering of emergent spin fluctuations in compressively strained $\text{La}_3\text{Ni}_2\text{O}_7$ on $\text{SrLaAlO}_4(001)$* (2025), [arXiv:2503.10902 \[cond-mat.supr-con\]](#).
- [61] G. Khaliullin and J. Chaloupka, *Orbital order and superconductivity in bilayer nickelate compounds* (2025), [arXiv:2506.16360 \[cond-mat.str-el\]](#).
- [62] H. Oh, H. Yang, and Y.-H. Zhang, *Doping a spin-one mott insulator: possible application to bilayer nickelate* (2025), [arXiv:2509.02673 \[cond-mat.str-el\]](#).
- [63] H. Yang, H. Oh, and Y.-H. Zhang, Strong pairing and symmetric pseudogap metal in a double kondo lattice model: From a nickelate superconductor to a tetralayer optical lattice, *Phys. Rev. B* **111**, L241102 (2025).
- [64] Y. Zhang, L.-F. Lin, A. Moreo, and E. Dagotto, Electronic structure, dimer physics, orbital-selective behavior, and magnetic tendencies in the bilayer nickelate superconductor $\text{La}_3\text{Ni}_2\text{O}_7$ under pressure, *Phys. Rev. B* **108**, L180510 (2023).
- [65] C. Lu, Z. Pan, F. Yang, and C. Wu, Interplay of two E_g orbitals in superconducting $\text{La}_3\text{Ni}_2\text{O}_7$ under pressure, *Phys. Rev. B* **110**, 094509 (2024).
- [66] X. Zhu, W. Qin, P. Cui, and Z. Zhang, *Quantum phase transition driven by competing intralayer and interlayer hopping of $ni-d_{3z^2-r^2}$ orbitals in bilayer nickelates* (2025), [arXiv:2507.11169 \[cond-mat.str-el\]](#).
- [67] Y. Zhang, L.-F. Lin, A. Moreo, T. A. Maier, and E. Dagotto, Electronic structure, self-doping, and superconducting instability in the alternating single-layer trilayer stacking nickelates $\text{La}_3\text{Ni}_2\text{O}_7$, *Phys. Rev. B* **110**, L060510 (2024).
- [68] L. Liu, H. Yao, E. Berg, S. R. White, and S. A. Kivelson, Phases of the infinite u hubbard model on square lattices, *Phys. Rev. Lett.* **108**, 126406 (2012).
- [69] Y.-B. Liu, H. Sun, M. Zhang, Q. Liu, W.-Q. Chen, and F. Yang, *Origin of the Diagonal Double-Stripe Spin-Density-Wave and Potential Superconductivity in Bulk $\text{La}_3\text{Ni}_2\text{O}_7$ at Ambient Pressure* (2025), [arXiv:2501.14752 \[cond-mat.supr-con\]](#).
- [70] Y. Wang, K. Jiang, Z. Wang, F.-C. Zhang, and J. Hu, *The electronic and magnetic structures of bilayer $\text{La}_3\text{Ni}_2\text{O}_7$ at ambient pressure* (2024), [arXiv:2401.15097 \[cond-mat.supr-con\]](#).
- [71] C. Zener, Interaction between the d -shells in the transition metals. ii. ferromagnetic compounds of manganese with perovskite structure, *Phys. Rev.* **82**, 403 (1951).
- [72] P. W. Anderson and H. Hasegawa, Considerations on double exchange, *Phys. Rev.* **100**, 675 (1955).
- [73] C. Lu, M. Zhang, Z. Pan, C. Wu, and F. Yang, Impact of pressure and apical oxygen vacancies on superconductivity in $\text{La}_3\text{Ni}_2\text{O}_7$, *Communications Physics* **8**, 354 (2025).
- [74] S. R. White, Density matrix formulation for quantum renormalization groups, *Phys. Rev. Lett.* **69**, 2863 (1992).
- [75] C. Hubig, I. P. McCulloch, U. Schollwöck, and F. A. Wolf, Strictly single-site dmrg algorithm with subspace expansion, *Phys. Rev. B* **91**, 155115 (2015).
- [76] E. Lieb and D. Mattis, Theory of ferromagnetism and the ordering of electronic energy levels, *Phys. Rev.* **125**, 164 (1962).
- [77] E. Lieb and D. Mattis, Ordering energy levels of interacting spin systems, *Journal of Mathematical Physics* **3**, 749 (1962).
- [78] J. Voit, An improved method for computing correlation functions of one-dimensional fermion systems, *Journal of Physics C: Solid State Physics* **21**, L1141 (1988).
- [79] T. Giamarchi and H. J. Schulz, Correlation functions of one-dimensional quantum systems, *Phys. Rev. B* **39**, 4620 (1989).
- [80] I. Affleck, D. Gepner, H. J. Schulz, and T. Ziman, Critical behaviour of spin-s heisenberg antiferromagnetic chains: analytic and numerical results, *Journal of Physics A: Mathematical and General* **22**, 511 (1989).
- [81] E. Dagotto, S. Yunoki, A. L. Malvezzi, A. Moreo, J. Hu, S. Capponi, D. Poilblanc, and N. Furukawa, Ferromagnetic kondo model for manganites: Phase diagram, charge segregation, and influence of quantum localized spins, *Phys. Rev. B* **58**, 6414 (1998).
- [82] D. Pekker, S. Mukhopadhyay, N. Trivedi, and P. M. Goldbart, Double-exchange model for noninteracting electron spins coupled to a lattice of classical spins: Phase diagram at zero temperature, *Phys. Rev. B* **72**, 075118 (2005).
- [83] S.-Q. Shen and Z. D. Wang, Phase separation and charge

- ordering in doped manganite perovskites: Projection perturbation and mean-field approaches, *Phys. Rev. B* **61**, 9532 (2000).
- [84] A. Chattopadhyay, A. J. Millis, and S. Das Sarma, $t = 0$ phase diagram of the double-exchange model, *Phys. Rev. B* **64**, 012416 (2001).
- [85] M. Sigrist, H. Tsunetsugu, K. Ueda, and T. M. Rice, Ferromagnetism in the strong-coupling regime of the one-dimensional kondo-lattice model, *Phys. Rev. B* **46**, 13838 (1992).
- [86] G. Honner and M. Gulácsi, One-dimensional kondo lattice at partial band filling, *Phys. Rev. Lett.* **78**, 2180 (1997).
- [87] G. Honner and M. Gulácsi, Ordering of localized moments in kondo lattice models, *Phys. Rev. B* **58**, 2662 (1998).
- [88] O. Zachar, S. A. Kivelson, and V. J. Emery, Exact results for a 1d kondo lattice from bosonization, *Phys. Rev. Lett.* **77**, 1342 (1996).
- [89] C. Santos and W. Nolting, Ferromagnetism in the kondo-lattice model, *Phys. Rev. B* **65**, 144419 (2002).
- [90] M. Gulacsi, A. Bussmann-Holder, and A. R. Bishop, Spin and lattice effects in the kondo lattice model, *Phys. Rev. B* **71**, 214415 (2005).
- [91] H. Tsunetsugu, M. Sigrist, and K. Ueda, The ground-state phase diagram of the one-dimensional kondo lattice model, *Rev. Mod. Phys.* **69**, 809 (1997).
- [92] R. Peters and N. Kawakami, Ferromagnetic state in the one-dimensional kondo lattice model, *Phys. Rev. B* **86**, 165107 (2012).
- [93] M. Troyer and D. Würtz, Ferromagnetism of the one-dimensional kondo-lattice model: A quantum monte carlo study, *Phys. Rev. B* **47**, 2886 (1993).
- [94] Note that in the presence of a finite coupling between $d_{x^2-y^2}$ and d_{z^2} orbitals (which has been neglected in our model), the $d_{x^2-y^2}$ Fermi surface will split into bonding and anti-bonding parts, on which the gap function changes sign, thus corresponding to s_{\pm} -wave pairing.